

Demonstration of local expansion toward large-scale entangled webs

Toshiyuki Tashima,¹ Tsuyoshi Kitano,¹ Şahin Kaya Özdemir,²
Takashi Yamamoto,¹ Masato Koashi,¹ and Nobuyuki Imoto¹

¹*Graduate School of Engineering Science, Osaka University, Toyonaka, Osaka 560-8531, Japan*

²*Department of Electrical and Systems Engineering,
Washington University, St. Louis, MO 63130 USA*

We demonstrate an optical gate that increases the size of polarization-based W states by accessing only one of the qubits. Using this gate, we have generated three-photon and four-photon W states with fidelities 0.836 ± 0.042 and 0.784 ± 0.028 , respectively. We also confirmed the existence of pairwise entanglement in every pair of qubits, including the one that was left untouched by the gate. The gate is applicable to any size of W states and hence is a universal tool for expanding entanglement.

PACS numbers: 03.67.Hk, 03.65.Ud

For the past two decades much effort has been devoted to the study of entanglement in order to grasp its nature [1] and to use it as a resource for various quantum information tasks such as quantum key distribution [2], quantum metrology [3], and quantum computing [4]. While entanglement between two quantum systems is well-understood, entanglement among three or more quantum systems still requires intense research effort. Even when we limit the constituent systems to the simplest ones, qubits, we still encounter many nonequivalent classes of entanglement which differ in the structure of how the qubits are correlated. In a Greenberger-Horne-Zeilinger (GHZ) state, the entanglement is sustained by all of the qubits [5], in the sense that removal of any one qubit completely disentangles the rest. Qubits in W states are entangled in the completely opposite way, where entanglement is compartmentalized such that entanglement between any pair of qubits survives after discarding the rest of the qubits [5–7]. Cluster states are halfway between the above two classes: Entanglement in the N -qubit linear cluster states is sustained by at least half of the qubits; that is, accessing $N/2$ qubits is enough to destroy the entanglement completely [8].

Recently, expansion gates have been introduced for preparing large-scale multipartite photonic entanglement [9–15]. In this approach, multipartite entangled states of a certain class are grown from a small seed by locally adding one or more qubits at a single site while retaining the structure of the desired entanglement class.

It is well known that GHZ states and cluster states are, in principle, deterministically expanded by applying a controlled-unitary gate between one of the entangled qubits and a fresh qubit to be added [9, 10]. Probabilistic implementations with linear optics based on quantum parity check have also been demonstrated [13–15]. The expansion of W states is much more complicated for several reasons. First of all, when we expand an N -qubit W state by accessing only one of the N qubits, the marginal state of the remaining $N - 1$ qubits must be changed to the proper state, which depends on the size of the ex-

panded larger W state. Thus, no unitary gates can be used for the expansion of W states, even in principle. Another complication arises from the difference in the structure of multipartite entanglement. As mentioned above, each pair of qubits in a W state sustain its own entanglement independently, resulting in a weblike structure of bonding among qubits [6, 7]. In order to expand an N -qubit W state while retaining such a structure, the newly added qubits should not only get entangled with the accessed qubit in the initial W state, but should also form independent pairwise entanglement with each of the untouched $N - 1$ qubits [see Fig. 1(a)].

In this Letter, we demonstrate an experimental implementation of this expansion task with a surprisingly simple gate. The gate shown in the dotted box of Fig. 1(b) is essentially composed of just two half beamsplitters with two-photon Fock states as a source of fresh qubits [11]. The gate involves three photons in total, including one photon from input mode 1 and two photons in H polarization in mode 2. The successful operation of the gate is defined to be the case where one photon emerges at each of the three output modes 4, 5, and 6. This gate can be used for the expansion of polarization-entangled W states written in the form

$$|W_N\rangle = \frac{1}{\sqrt{N}} \sum_{j=1}^N a_{jV}^\dagger \left(\prod_{i \neq j} a_{iH}^\dagger \right) |vac\rangle \quad (1)$$

where $|vac\rangle$ denotes the vacuum state for all modes and $a_{iV(H)}^\dagger$ is the creation operator of a V (H)-polarized photon in mode i . The gate is size independent; namely, the same gate is applicable to the expansion of an N -qubit polarization-based W state of any size N to produce an $N + 2$ -qubit polarization-based W state. In this case, the photon in mode 1 is provided by the N -photon polarization-based W state. Here we present an experimental demonstration of the gate to prepare three- and four-photon polarization-based W states corresponding to $N = 1$ and $N = 2$, respectively.

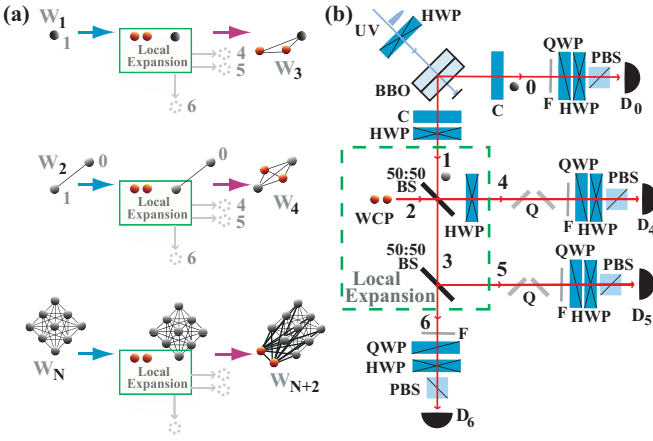


FIG. 1: (a) Concept of local state expansion. (b) Experimental setup. BBO: β -barium borate crystals (thickness 1.5mm + 1.5mm). HWP: half-wave plate. QWP: quarter-wave plate. UV: ultraviolet pulse. BS: beamsplitter. IF: narrowband interference filter (wavelength 790nm, bandwidth 2.7nm). Q: quartz crystals. C: BBO (thickness 1.65mm) used to compensate walk-off effects. Although the ideal operation of the gate requires two-photon Fock state in mode 2, in the experiments the two photons of mode 2 are provided by a weak coherent pulse (WCP). All the detectors ($D_{0,4,5,6}$) are silicon avalanche photodiodes placed after single-mode optical fibers.

In the following, we will briefly explain the working principle of the expansion gate depicted in the dotted box in Fig. 1(b). Let us first consider the case where the input photon is V polarized, namely, state $|1_V\rangle_1 \equiv \hat{a}_{1_V}^\dagger |vac\rangle_1$, where $|vac\rangle_1$ stands for the vacuum for mode 1. This photon is distinguishable from the two photons of mode 2 in state $|2_H\rangle_2$ by polarization. Hence the classical particle picture is applicable, namely, V, H, and H photons emerge at modes 4, 5, and 6, respectively, with a probability of 1/16. The successful operation involves the other two cases, HVH and HHV, too. The relevant state transformation for the two beam splitters (BSs) is thus written as

$$|1_V\rangle_1 \rightarrow \frac{1}{4}[-|1_V\rangle_4|1_H\rangle_5|1_H\rangle_6 + |1_H\rangle_4|1_V\rangle_5|1_H\rangle_6 + |1_H\rangle_4|1_H\rangle_5|1_V\rangle_6], \quad (2)$$

where the minus sign appears when the photon in mode 1 is reflected toward mode 4. The half wave-plate (HWP) in mode 4 is used to compensate this sign by introducing a π phase shift on the V polarization. The transformation by the entire gate is thus given by

$$|1_V\rangle_1 \rightarrow \frac{1}{4}[|1_V\rangle_4|1_H\rangle_5|1_H\rangle_6 + |1_H\rangle_4|1_V\rangle_5|1_H\rangle_6 + |1_H\rangle_4|1_H\rangle_5|1_V\rangle_6] = \frac{\sqrt{3}}{4}|W_3\rangle, \quad (3)$$

which means that a V-polarized photon is expanded to a three-photon W state with a probability of 3/16.

When the input photon in mode 1 has H polarization, the transformation is simply given by changing V to H in Eq. (2). Since the HWP has no effect, this leads to

$$|1_H\rangle_1 \rightarrow \frac{1}{4}|1_H\rangle_4|1_H\rangle_5|1_H\rangle_6. \quad (4)$$

Here the success probability is reduced by a factor of 3, due to the destructive interference caused by the indistinguishability of photons.

The transformation for a general input is now calculated from Eqs. (3) and (4). When the input is one photon of the bipartite entangled state $|W_2\rangle \equiv (|1_H\rangle_0|1_V\rangle_1 + |1_V\rangle_0|1_H\rangle_1)/\sqrt{2}$, this gate performs the transformation $|W_2\rangle \rightarrow (1/\sqrt{8})|W_4\rangle$ resulting in a four-partite W state with a probability of 1/8. Note that the photon in mode 0 of $|W_2\rangle$ is untouched by this gate. When the input photon in mode 1 is provided by an N -photon W state, the gate performs the transformation $|W_N\rangle \rightarrow \sqrt{(N+2)/16N}|W_{N+2}\rangle$. Hence the gate is applicable to any N , with a success probability of $(N+2)/(16N)$.

Our experimental setup designed for the realization of this gate is shown in Fig. 1(b). The light pulses from a mode-locked Ti:sapphire laser (wavelength 790nm, pulse width 90fs, repetition rate 82MHz) are divided into two unequal parts by a tilted glass plate. The weak portion is used to prepare an H-polarized weak coherent pulse (WCP) with adjustable mean photon number $\nu \ll 1$. With a probability of $\sim \nu^2/2$, this pulse includes two photons, which are used as the ancillary state $|2_H\rangle$. The strong portion goes to a second harmonic generator to prepare the ultraviolet (UV) pulse used for photon pair generation by a spontaneous parametric down conversion (SPDC) in Type I phase matched β -barium borate (BBO) crystals stacked together with their optical axes orthogonal to each other [16]. The photon pair generation rate γ is adjusted such that $\gamma \ll \nu \ll 1$ is satisfied. This ensures that the events with the WCP having one photon make little contribution to the coincidence detection.

As a preliminary experiment, we made sure that a single photon from SPDC was in a well-matched mode with the WCP when they were overlapped at the first 50:50 BS. V-polarized UV pump pulses of an average power 23 mW are used for the SPDC, and detection of one H photon in mode 0 prepares an H-polarized single photon in mode 1. The H-polarized WCP in mode 2 is set to have $\nu = 0.03$. The three-fold coincidences at modes 0, 4, and 5 were recorded while varying the delay at mode 2 using a motorized stage. A Hong-Ou-Mandel dip with visibility 0.85 at zero delay was observed [see Fig. 2]. This indicates a good overlap between the two modes.

As a demonstration of our expansion gate, we first fed a V-polarized single photon ($|W_1\rangle$) to the gate to produce $|W_3\rangle$. The V-polarized single photon is prepared by rotating the polarization of the single photon pre-

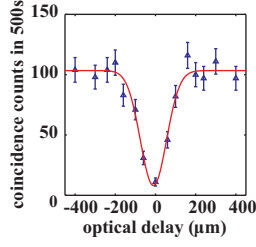


FIG. 2: Observed two-photon interference. The best fit to the experimental data is represented by the solid Gaussian curve (coherence length $l_c \simeq 144\mu\text{m}$ and visibility is 0.85).

pared in the preliminary experiment by $\pi/2$ using the HWP at mode 1. The successful operation of the gate is post-selected by the four-fold coincidence detection at modes 4, 5, 6, and 0. We set $\nu = 0.3$ for the WCP and an average power of 75 mW for the UV pump, and reconstruct the density matrix ρ_{456} of the three photons at modes 4, 5, and 6 using the iterative maximum likelihood method (IMLM) from the polarization-correlation measurements on 64 different settings formed by combinations of the single photon projections to $|H\rangle$, $|V\rangle$, $|D\rangle = (|H\rangle + |V\rangle)/\sqrt{2}$, $|R\rangle = (|H\rangle - i|V\rangle)/\sqrt{2}$, and $|L\rangle = (|H\rangle + i|V\rangle)/\sqrt{2}$ [17, 18]. The coincidences were recorded for an acquisition time of 5220s at each tomographic setting with a typical fourfold coincidence rate of ~ 0.02 counts/s. The reconstructed density matrix ρ_{456} shown in Fig. 3(a) carries a similar structure as the ideal $|W_3\rangle$ which consists of only nine real and nonzero terms, namely, the diagonal terms corresponding to $|HHV\rangle$, $|H VH\rangle$ and $|VHH\rangle$ and six off-diagonal elements corresponding to coherence among these terms. Fidelity of the output state to $|W_3\rangle$ is calculated as $F_{456} \equiv \langle W_3 | \rho_{456} | W_3 \rangle = 0.836 \pm 0.042$, and the expectation value of the entanglement witness operator $\mathcal{W}_W = \frac{2}{3}\mathbf{1} - |W_3\rangle\langle W_3|$ is calculated as $\text{Tr}(\mathcal{W}_W \rho_{456}) = -0.169 \pm 0.042$, whose negativity proves that the prepared state has genuine tripartite entanglement [19, 20]. In order to confirm the presence of the pairwise entanglement in the prepared W state, we calculated the marginal density matrices of pairwise combinations ρ_{45} , ρ_{46} and ρ_{56} from the reconstructed state ρ_{456} and depicted them in Fig. 3(b). We also calculated the values of entanglement of formation (EOF) as $\mathcal{E}(\rho_{45}) = 0.354 \pm 0.070$, $\mathcal{E}(\rho_{46}) = 0.273 \pm 0.065$ and $\mathcal{E}(\rho_{56}) = 0.316 \pm 0.074$, respectively [21]. All pairwise components of the output state ρ_{456} enjoy entanglement, demonstrating that the state expansion gate acts as an entangling gate and expands a single photon state into a tripartite W state. These results imply that the transformation given in Eq. (3) has been performed successfully in our experiments.

Next we proceed to the expansion of a bipartite entangled state ($|W_2\rangle$) into $|W_4\rangle$. By setting the polarization of UV pulses (average power: 150mW) to diagonal po-

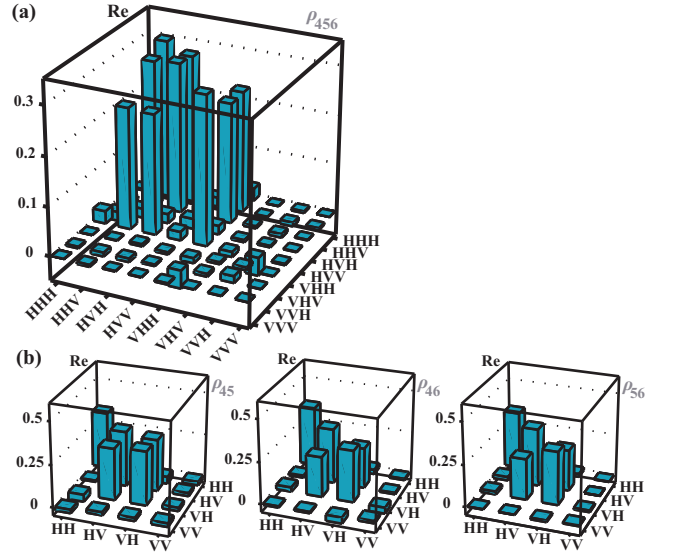


FIG. 3: Results of the expansion of $|W_1\rangle$ to a three-photon polarization-entangled W state $|W_3\rangle$. (a) The real part of the reconstructed density matrix of the final state ρ_{456} . (b) The real parts of the reconstructed reduced density matrices ρ_{45} , ρ_{46} , and ρ_{56} .

larization, we prepared the bipartite entangled state σ_{01} and characterized it by reconstructing its density matrix by measuring polarization correlations in modes 0 and 6 using 16 different basis settings. Fidelity to a maximally entangled photon pair $F_{01} \equiv \langle W_2 | \sigma_{01} | W_2 \rangle$ and the EOF of the prepared state are calculated as $F_{01} = 0.977 \pm 0.005$ and $\mathcal{E}(\sigma_{01}) = 0.964 \pm 0.013$, respectively, confirming that the prepared state is a highly entangled photon pair. Then we mixed the photon in mode 1 of σ_{01} with the WCP ($\nu = 0.3$) and post-selected the successful events by fourfold coincidences in modes 0, 4, 5 and 6. The state σ_{0456} of the four photons was reconstructed using 256 different tomographic settings. The coincidences were recorded for an acquisition time of 4280s at each tomographic setting with a typical fourfold coincidence rate of ~ 0.02 counts/s. The density matrix of σ_{0456} was reconstructed using the IMLM (Fig. 4(a)). The density matrix of an ideal $|W_4\rangle$ state consists of 16 real and nonzero elements including twelve off-diagonal elements depicting the coherences among the four diagonal terms $|HHHV\rangle$, $|HHVH\rangle$, $|HVHH\rangle$ and $|VHHH\rangle$. A similar structure is clearly seen in the density matrix of the output state σ_{0456} of the expansion gate. From the reconstructed density matrix, we calculated the fidelity as $F_{0456} \equiv \langle W_4 | \sigma_{0456} | W_4 \rangle = 0.784 \pm 0.028$. The entanglement witness calculated using the operator $\mathcal{W}_W = \frac{3}{4}\mathbf{1} - |W_4\rangle\langle W_4|$ has the ideal expectation value of $-1/4$ for an ideal $|W_4\rangle$ [20]. The presence of genuine four-partite entanglement in σ_{0456} is confirmed by the calculated expectation value of $\text{Tr}(\mathcal{W}_W \sigma_{0456}) = -0.034 \pm 0.028$.

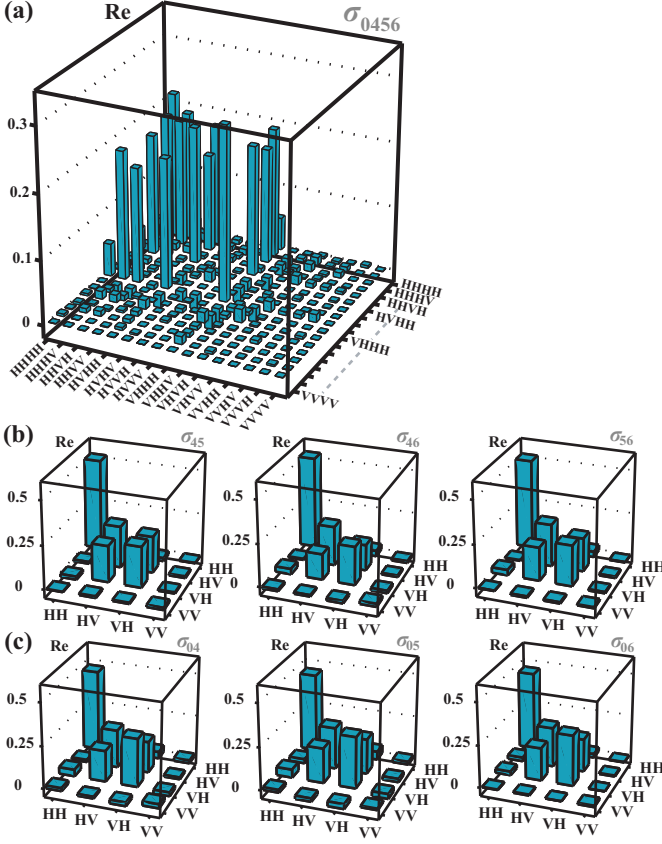


FIG. 4: Results of the expansion of $|W_2\rangle$ to a four-photon polarization-entangled W state $|W_4\rangle$. (a) The real part of the reconstructed density matrix of the final state σ_{0456} . (b) The real parts of the reconstructed reduced density matrices σ_{045} , σ_{046} , and σ_{056} , and (c) those of σ_{004} , σ_{005} , and σ_{006} .

It is known that the larger the W state, the weaker the pairwise entanglement, which makes it more challenging to observe experimentally. We have calculated two-qubit marginal density operators for various combinations of the reconstructed density operator σ_{0456} . Figure 4(b) shows the three combinations for the qubits 4, 5 and 6, which have been directly interacted at the gate. The calculated values of EOF for these cases are $\mathcal{E}(\sigma_{45}) = 0.040 \pm 0.022$, $\mathcal{E}(\sigma_{46}) = 0.167 \pm 0.033$ and $\mathcal{E}(\sigma_{56}) = 0.133 \pm 0.030$, which are all positive. Figure 4(c) shows the two-qubit density operators involving the photon in mode 0, which has been untouched by the gate. The calculated values of the EOF are all positive: $\mathcal{E}(\sigma_{04}) = 0.184 \pm 0.037$, $\mathcal{E}(\sigma_{05}) = 0.072 \pm 0.028$ and $\mathcal{E}(\sigma_{06}) = 0.146 \pm 0.033$. Although experimentally achieved EOF are smaller than the theoretical maximum of 0.35, they are a conclusive sign of the presence of pairwise entanglement in every pair, which is the crucial property of $|W_4\rangle$. This result also confirms that the transformations in Eqs. (3) and (4) were carried out coherently in our experiment.

If we interpret that the photon in mode 1 has come

out in mode 4 after the interaction with the two photons in mode 2, we may say that the pairwise entanglement in σ_{05} and σ_{06} were newly created as a result of the gate operation, while the original strong entanglement $\mathcal{E}(\sigma_{01}) = 0.95 \pm 0.02$ was reduced to $\mathcal{E}(\sigma_{04}) = 0.15 \pm 0.03$. One may also argue that the three photons 4, 5, and 6 are indistinguishable, and hence none of them are entitled to be the exclusive descendant of the photon in mode 1. This picture gives rise to another interesting interpretation, in which the photon in mode 1 has been cloned into the three copies, 4, 5, and 6. In contrast to the conventional $1 \rightarrow 3$ optimal cloning in which the only aim is to copy the state (including correlations to a reference system) of the input qubit as good as possible [22], our gate produces pairwise entanglement among the three output qubits, in addition to the conventional task. The gate is optimal in achieving both of the tasks, which comes from the optimality of the pairwise entanglement in $|W_4\rangle$. Figures 4(b) and 4(c) show that both of the tasks are achieved at the same time in our experiment.

In summary, we have shown that the size of a multipartite entanglement can be expanded by operating a simple gate on one local site, preserving the characteristic entanglement structure over the whole system including the sites to which the gate has no access. We demonstrated expansion of W states up to the size of four, and the same gate is expected to be applicable to any size of W states. Thanks to the simple structure, the expansion gate can be easily miniaturized by integration on recently developed silicon waveguide quantum circuits [23]. We believe that the demonstrated expansion gate has the potential to become an integral part of any quantum optical toolbox aimed at the preparation, manipulation and understanding of multipartite entangled states.

This work was supported by the Funding Program for World-Leading Innovative R&D on Science and Technology (FIRST), MEXT Grant-in-Aid for Scientific Research on Innovative Areas No. 20104003 and No. 21102008, JSPS Grant-in-Aid for Scientific Research(C) No. 20540389, and MEXT Global COE Program.

-
- [1] R. Horodecki, *et al.*, Rev. Mod. Phys. **81**, 865 (2009).
 - [2] A. K. Ekert, Phys. Rev. Lett. **67**, 661 (1991).
 - [3] T. Nagata *et al.* Science **316**, 726 - 729 (2007).
 - [4] M. A. Nielsen and I. L. Chuang, "Quantum Computation and Quantum Information", Cambridge university Press, Cambridge, England, (2000).
 - [5] W. Dür, G. Vidal, and J. I. Cirac, Phys. Rev. A **62**, 062314 (2000).
 - [6] M. Koashi, V. Bužek, and N. Imoto, Phys. Rev. A **62**, 050302(R) (2000).
 - [7] W. Dür, Phys. Rev. A **63**, 020303(R) (2001).
 - [8] H. J. Briegel and R. Raussendorf Phys. Rev. Lett. **86**, 910 (2001).
 - [9] T. B. Pittman, B. C. Jacobs, and J. D. Franson, Phys.

- Rev. A **64**, 062311 (2001).
- [10] M. A. Nielsen, Phys. Rev. Lett. **93**, 040503 (2004).
 - [11] T. Tashima *et al.* Phys. Rev. A **77**, 030302(R) (2008).
 - [12] T. Tashima *et al.* New J. Phys **11**, 023024 (2009). Y-X. Gong, X-B. Zou, Y-F. Huang, and G-C.Guo, J. Phys. B: At. Mol. Opt. Phys **42**, 035503 (2009).
 - [13] Z. Zhao, *et al.* Nature (London) **430**, 54 - 58 (2004).
 - [14] K. J. Resch, P. Walther and A. Zeilinger, Phys. Rev. Lett. **94**, 070402 (2005).
 - [15] C. Y. Lu, *et al.* Nature Physics **3**, 91 - 95 (2007).
 - [16] P. G. Kwiat, *et al.* Phys. Rev. A **60**, R773 (1999).
 - [17] D. F. V. James, *et al.* Phys. Rev. A **64**, 052312 (2001).
 - [18] J. Řeháček, Z. Hradil, and M. Ježek, Phys. Rev. A **63**, 040303(R) (2001).
 - [19] M. Bourennane *et al.* Phys. Rev. Lett. **92**, 087902 (2004).
 - [20] O. Gühne, and G. Toth, Physics Reports **474**, 1 (2009).
 - [21] W. K. Wootters, Phys. Rev. Lett. **80**, 2245 (1998).
 - [22] V. Bužek, and M. Hillery, Phys. Rev. A **54**, 1844 (1996). N. Gisin, and S. Massar, Phys. Rev. Lett. **79**, 2153 (1997).
 - [23] A. Politi, *et al.* Science **320**, 646 - 649 (2008).